CHEMISTRY
A EUROPEAN JOURNAL

DOI: 10.1002/chem.200701310

Precursor Approach to Lanthanide Dioxo Monocarbodiimides $Ln_2O_2CN_2$ (Ln = Y, Ho, Er, Yb) by Insertion of CO_2 into Organometallic Ln–N Compounds

Martin Zeuner, Sandro Pagano, and Wolfgang Schnick*[a]

Abstract: We present two organometallic precursor approaches leading to the hitherto-unknown dioxo monocarbodiimides ($Ln_2O_2CN_2$) of the late lanthanides Ho, Er, and Yb as well as yttrium. One involves insertion of CO_2, and the other one is a straightforward route using a molecular single-source precursor. To this end the reactivity of the activated amido lanthanide compound $[(Cp_2ErNH_2)_2]$ towards carbon dioxide absorption under supercritical conditions was studied. Selective insertion of CO_2 into the amido complex yielded the single-source precursor $[Er_2(O_2CN_2H_4)Cp_4]$, which was characterized by vibrational spectroscopy and thermal and elemental analyses. Ammonolysis of this amorphous compound at 700 °C affords $Er_2O_2CN_2$. To gain deeper insight into the structural characteristics of the amorphous precursor, a similar molecular carbamato complex was synthesized and fully characterized. X-ray structure analysis of the dimeric complex $[Cp_4Ho_2\{\mu\text{-}\eta^1\text{:}\eta^2\text{-}OC(O\textit{t}Bu)NH\}]$ shows an unusual bonding mode of the *tert*-butylcarbamate ligand, which acts as both a bridging and side-on chelating group. Ammonolysis of this compound also yielded dioxo monocarbodiimides, and therefore the crystalline carbamato complex turned out to be an alternative precursor for the straightforward synthesis of $Ln_2O_2CN_2$. Analogously, the dioxo monocarbodiimides of Y, Ho, Er, and Yb were synthesized by this route. The crystal structures were determined from X-ray powder diffraction data and refined by the Rietveld method (Ln = Ho, Er). Further spectroscopic characterization and elemental analysis evidenced the existence of phase-pure products. The dioxo monocarbodiimides of holmium and erbium crystallize in the trigonal space group $P\bar{3}m1$. According to X-ray powder diffraction, they adopt the $Ln_2O_2CN_2$ (Ln = Ce–Gd) structure type.

Keywords: carbamato ligands · carbon dioxide fixation · lanthanides · solid-phase synthesis · supercritical fluids

Introduction

In the last few years, oxidic and nitridic lanthanide-containing materials have received considerable attention due to their outstanding properties, which mainly originate from the f-elements.[1] Numerous applications in heterogeneous and homogeneous catalysis,[2–4] semi- and superconductivity,[5–7] and the development of novel phosphor materials for application in highly efficient white-light-emitting phosphor-converted (pc) LEDs have been reported.[8,9] Hence, there is a strong demand for new routes towards nitrogen-containing lanthanide compounds which are useful precursors in solid-state synthesis. On this background we are targeting simple molecular precursor compounds with ligands exhibiting an adequate thermal lability for subsequent pyrolysis reactions. The reaction of Cp_3Ln complexes (Ln = Sm, Dy, Ho, Er, Yb) with liquid ammonia yielded sublimable ammine complexes. Thermal treatment of these ammine complexes yielded the respective dimeric amido complexes **1** [Eqs. (1) and (2); Ln = Dy, Ho, Er, Yb]. Characterization and thermal degradation of the latter yielding nanocrystalline LnN solids has recently been reported.[10,11]

Partial substitution of O by N in lanthanide-containing Si/N materials (nitridosilicates)[12–14] allowed tailor-made tuning of luminescent properties for industrial application of these

$$Cp_3Ln + NH_3 \xrightarrow{-78\,^\circ C} Cp_3LnNH_3 \quad (1)$$

$$2\,Cp_3LnNH_3 \xrightarrow{\Delta} \underset{\mathbf{1}}{[(Cp_2LnNH_2)_2]} + 2\,CpH \quad (2)$$

[a] M. Zeuner, S. Pagano, Prof. Dr. W. Schnick
Ludwig-Maximilians-Universität
Department Chemie und Biochemie
Butenandtstrasse 5–13 (D), 81377 München (Germany)
Fax: (+49) 89-2180-77440
E-mail: wolfgang.schnick@uni-muenchen.de

Supporting information for this article is available on the WWW under http://www.chemeurj.org/ or from the author.

compounds.[8,9] Therefore, it is intriguing to integrate oxygen into C/N compounds (e.g., nitridocarbonates). During our studies on the reactivity of lanthanide amine and amido complexes towards CO_2, we synthesized a number of O/C/N-containing precursors.[15] Our studies revealed the formation of amorphous carbamate-containing compounds. The present study corroborates the controllable formation of Ln/O/C/N-containing single-source precursors by absorption and fixation of CO_2. Carbon dioxide was used as a preorganized C/O donor forming labile carbamate intermediates. These compounds turned out to be excellent starting materials for the synthesis of hitherto unavailable species in the system Ln/O/C/N. Lanthanide dioxo monocarbodiimides $Ln_2O_2CN_2$ (Ln = La–Gd) have been known since 1995 and were originally synthesized by treating the oxides with a stream of NH_3 at 950 °C in a graphite crucible.[16,17] Two different structure types have been reported, both of which consist of $[Ln_2O_2]^{2+}$ layers. $La_2O_2CN_2$ crystallizes with a tetragonal lattice in which La is coordinated by four oxygen and four nitrogen atoms. As a result of the smaller ionic radii the following lanthanides (Ce–Gd) are coordinated by four oxygen and three nitrogen atoms in a trigonal lattice. The closely related lanthanide oxo sulfides are of relevance as phosphors for cathode ray tube (CRT) phosphors and X-ray scintillators.[18,19] Therefore doped lanthanide dioxo monocarbodiimides have attracted much attention.[20–23] This is due to the fact that the presence of $[Ln_2O_2]^{2+}$ layers in the structure may be responsible for interesting luminescence properties.[24] To increase the doping range new synthetic pathways involving a sol–gel method were studied.[25] However, attempts to synthesize lanthanide dioxo monocarbodiimides of the heavy rare earth elements have yet not been successful. By studying metathesis reactions between lanthanide chlorides and lithium cyanamide Meyer et al. were recently able to obtain $Y_2O_2CN_2$[26] as well as the second formula type in the system Ln/O/C/N with composition $La_2O(CN_2)_2$.[27] These recent results and the rapidly growing chemistry of main group[28–30] and transition metal[31,32] carbodiimides underline the increasing interest in materials based on nitrido- and oxonitridocarbonates.

Here we report two organometallic pathways towards phase-pure synthesis of the heavy lanthanide dioxo monocarbodiimides, one of which involves insertion of CO_2 into the amido complex $[(Cp_2ErNH_2)_2]$ (**1**) to form the single-source precursor $[Er_2(O_2CN_2H_4)Cp_4]$ (**2**). To provide a deeper insight into the structural characteristics of the carbamate precursor, the crystalline carbamato complex $[Cp_4Ho_2\{\mu\text{-}\eta^1\text{:}\eta^2\text{-}OC(O\mathit{t}Bu)NH\}]$ (**3**) was synthesized and fully characterized. After ammonolysis, both precursors yielded the thus far unknown dioxo monocarbodiimides of Er and Ho.

Results and Discussion

Heterogeneous solid–gas reaction of 1 in supercritical CO_2: We investigated the insertion of CO_2 into lanthanide amido compounds under various reaction conditions.[15] The use of supercritical CO_2 ($scCO_2$) allows reactions to be carried out in "liquid" carbon dioxide under mild reaction conditions. To investigate the dependence of CO_2 insertion on temperature and pressure, **1** was transferred to a pressure vessel and brought to reaction with $scCO_2$ at 50 °C and 150 °C. The solids were analyzed by elemental analysis, thermal analysis, and IR spectroscopy. The IR spectra of the carboxylation products and of ammonium carbamate are depicted in Figure 1.

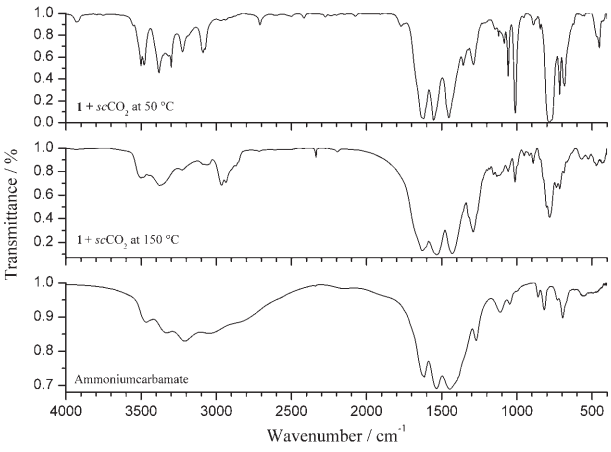

Figure 1. FTIR spectra of the carboxylation product of **1** after reaction in supercritical CO_2 (top: $T = 50$ °C, $p = 220$ bar; middle: $T = 150$ °C, $p = 220$ bar) and ammonium carbamate[15] (bottom).

The carboxylation product obtained at 50 °C still shows the typical stretching and deformation vibrations of the cyclopentadienyl ligands at 3088, 3070, 1357, 1010, 783, and 773 cm^{-1},[33,34] that is, degradation and elimination of the Cp rings has not occurred. This is probably due to the mild reaction conditions of $scCO_2$ at 50 °C. The bands at 3381, 3300, and 3225 cm^{-1} can be identified as the N–H stretching vibrations of the amido group. In contrast the carboxylation product obtained at 150 °C shows a broadening of the vibrational bands and a significant degradation of the Cp ligands, as evidenced by the decrease of the bands at 1013 and 782 cm^{-1} and the absence of that at 3088 cm^{-1}. This may be due to thermal degradation, but it more likely indicates that CO_2 insertion into the Er–C bond has occurred. Such an insertion into the Ln–C bond and formation of a carboxylato complex has been observed by Evans et al.[35] The absorptions at 1013 and 782 cm^{-1} are related to the Er–Cp (out-of-plane and in-plane wagging)[36] vibrations. Insertion of CO_2 into the Er–C bond increases the distance to the ligands and hence decreases the intensity of these vibrations. Furthermore, broadening of the N–H stretching vibrations indicate N–H··N hydrogen bonds between the molecular units in the solid and thus cross-linking between the molecules to form a polymeric product.[37] The spectrum of ammonium carbamate also shows very broad N–H and O–H vibrational bands due to hydrogen-bonded carbonyl and ammonium moieties. The spectra have three strong bands between 1650

and 1400 cm^{-1} in common (Figure 1). They are assigned to the C=O and C=N moieties of carbamato derivatives.[38]

Due to their similar shape and nearly identical absorption pattern to the IR spectrum of ammonium carbamate, the formation of carbamate complexes is highly probable.

Elemental analysis of the carboxylation product obtained at 50 °C suggested the composition Er/O/C/N/H = 2/2/21/2/24 corresponding to the formula $[Er_2(O_2CN_2H_4)Cp_4]$ (**2**). The elemental analysis corroborates the insertion of one carbon dioxide molecule per dimeric amido complex forming a carbamate moiety.

In contrast, the elemental analysis of the carboxylation product obtained at 150 °C exhibits a composition of Er/O/C/N/H = 2/10/25/2/24. The resulting formula $[Er_2(O_2CNH_2)_2(CO_2)_3Cp_4]$ corresponds to five CO_2 molecules per dimeric complex. This extensive coordination of oxygen at the metal center results in a product which is transformed into Er_2O_3 by pyrolysis.

These results demonstrate that the amount of CO_2 inserted into the complexes is predominantly dependent on the reaction temperature if the pressure is held constant. Furthermore, the findings highlight the importance of adding one equivalent of CO_2 per amido complex in order to obtain useful carbamate precursors and to avoid the formation of lanthanide oxides during subsequent pyrolysis reactions.

The reaction of **1** in $scCO_2$ at 50 °C is shown in Equation (3).

$$\underset{\mathbf{1}}{[(Cp_2ErNH_2)_2]} + scCO_2 \xrightarrow[220\ bar]{50\ °C} \underset{\mathbf{2}}{[Er_2(O_2CN_2H_4)Cp_4]} \qquad (3)$$

We are particularly interested in thermally induced cleavage and elimination of the Cp ligands to obtain a deeper insight into the reaction conditions required for the preparation of highly condensed and defined inorganic solids.

Thermogravimetric/differential thermal analysis (TG/DTA) measurements on **2** between 25 and 1400 °C were supported by in situ mass spectrometry of the gaseous pyrolysis products. In contrast to pyrolysis of **2** in gaseous ammonia affording $Er_2O_2CN_2$, the TG/DTA measurements were carried out under He atmosphere and yielded an amorphous residue. This underlines the importance of using a reductive atmosphere to obtain carbodiimides from carbamate precursors. Nevertheless, coupling of TG/DTA with in situ mass spectrometry provides useful information about the degradation process. The ion flow exhibits one strong, broad maximum at 147 °C related predominantly to elimination of Cp ligands. CO_2 as a pyrolysis product was observed between 50 and 500 °C. However, in the temperature range before and after 147 °C the MS only shows signals of CO_2. This is consistent with fast and complete loss of all Cp ligands to leave a residue which continuously releases CO_2 under a nonreducing atmosphere.

Differential scanning calorimetry (DSC) measurements on **2** at a heating rate of 5 °C min^{-1} in a closed aluminum crucible revealed two weak and one broad endothermic signals at 166, 200, and 233 °C, respectively (Figure 2).

The broad signal at 233 °C can be attributed to loss of the Cp rings. DSC and TG/DTA measurements on **2** indicate differences in thermal behavior; the higher degradation temperature results from the different pressure conditions of the DSC and TG/DTA measurements.

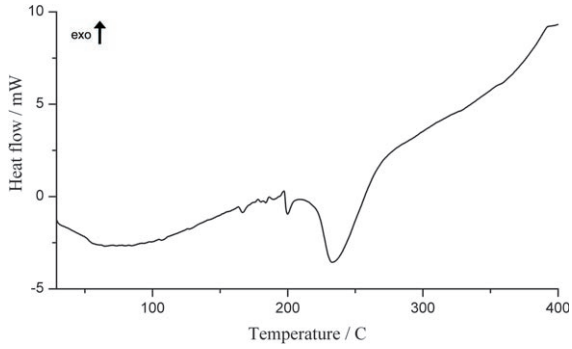

Figure 2. Differential scanning calorimetry of **2** between room temperature and 400 °C. The significant thermal event at 233 °C can be attributed to loss of the Cp rings.

Pyrolysis of 2: To achieve complete cleavage and elimination of the organic ligands and thereupon force the precursor to condense, pyrolysis under a stream of dry ammonia was studied. To this end, a special Schlenk line with ammonia dried over Na and K was employed. The results from TG/DTA measurements under inert gas indicate the onset of thermal decomposition of the organic ligands at 122 °C. Under ammonia atmosphere the temperature must exceed 250 °C to achieve significant mass loss, which is consistent with the DSC measurements. Consequently, **2** was pyrolyzed at 250 °C to remove the organic moieties.

Subsequent thermal treatment of the product of the reaction up to 700 °C under NH_3 atmosphere resulted in formation of a black solid, which showed a broadened diffraction pattern similar to that of trigonal $Ln_2O_2CN_2$ (Ln = Ce–Gd). To obtain higher crystallinity a LiCl/KCl flux was applied by analogy to recent reports in lanthanide carbodiimide chemistry.[27,39,40] After the first decomposition stage at 250 °C the product was mixed with a eutectic mixture of LiCl and KCl. After annealing at 700 °C, a gray-purple product was obtained. X-ray powder diffraction (XRPD) patterns indicated formation of a highly crystalline solid. Formation of hexagonal platelets was observed by scanning electron microscopy (SEM). An SEM image of the reaction product after separation from the LiCl/KCl flux is depicted in Figure 3.

With the structural model of $Eu_2O_2CN_2$,[16] the structure of $Er_2O_2CN_2$ was refined by the Rietveld method with the program GSAS.[41] Figure 4 depicts the Rietveld plot of $Er_2O_2CN_2$. Details of the structure determination are summarized in Table 1. The atom positions and isotropic displacement parameters can be found in the Supporting Information.

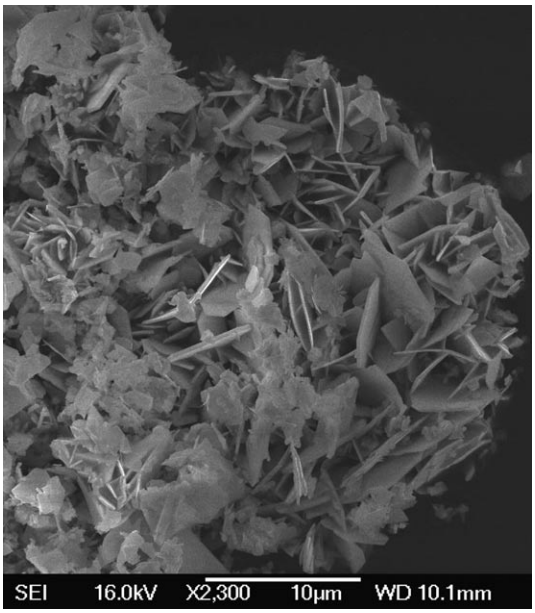

Figure 3. Scanning electron microscopy image of $Er_2O_2CN_2$.

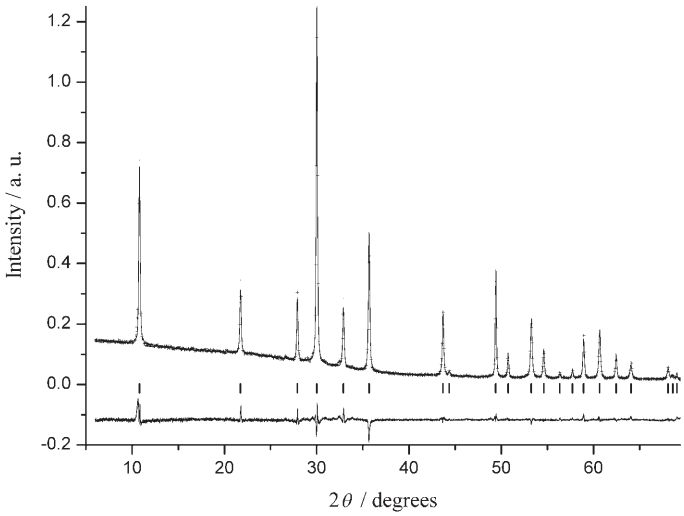

Figure 4. Final Rietveld refinement plot for $Er_2O_2CN_2$. Observed (+), calculated (line), and difference profile of the X-ray powder diffraction are plotted on the same scale. Bragg peaks for $Er_2O_2CN_2$ are indicated by vertical lines.

FTIR spectroscopic investigations of $Er_2O_2CN_2$ show the typical two absorption bands for carbodiimides: ν_{as} and ν_s at 2157 and 652 cm^{-1}, respectively. Compared to the IR data of the early lanthanide dioxo monocarbodiimides,[16] the vibrational frequencies of the ν_{as} band increase with decreasing radii of the corresponding cations. An analogous effect has been observed in the spectroscopic data of the alkaline earth metal cyanamides and can be explained by the reciprocal relation between the polarization of the nitrogen atoms and the size of the cations. This polarization reduces the repulsion between the lone pairs of the nitrogen atoms. Consequently, the antibonding interactions decrease and the C–N bonding is stabilized.[29,42]

Table 1. Results of the Rietveld refinement of $Er_2O_2CN_2$ and $Ho_2O_2CN_2$.

	$Er_2O_2CN_2$	$Ho_2O_2CN_2$
formula weight	406.54	401.88
crystal system	trigonal	
space group	$P\bar{3}m1$ (No. 164)	
radiation (λ [Å])	$Cu_{K\alpha1}$ (1.5406)	
a [Å]	3.67440(5)	3.70424(3)
c [Å]	8.13371(17)	8.16923(13)
V [Å^3]	95.104(3)	97.07(3)
Z	1	1
ρ_{calcd} [g cm^{-3}]	7.10	6.87
diffractometer	STOE Stadi P	Huber G670
θ range [°]	$3 \le \theta \le 35.02$	$3 \le \theta \le 43.95$
structure parameters	5	5
background function	shifted Chebyshev	
coefficients	12	32
wR_p (fitted)	0.0617	0.0296
wR_p (background)	0.1397	0.0643
R_p (fitted)	0.0399	0.0197
R_p (background)	0.0591	0.0438
χ^2	3.521	1.477
R_F^2	0.0941	0.0470

Due to the large mass difference between the lanthanide and the carbodiimide it is an intrinsic problem to obtain precise information about the C–N bond lengths; therefore, the C–N bond had to be held at 1.22 Å.

Elemental analysis of the ammonolysis product indicated a composition of Er/O/C/N = 2/2/1/2. The resulting formula $Er_2O_2CN_2$ supports the formation of phase-pure erbium dioxo monocarbodiimide.

In summary the degradation step can be represented by Equation (4).

$$\underset{\mathbf{2}}{[Er_2(O_2CN_2H_4)Cp_4]} \xrightarrow[NH_3\ (g.)]{700\ ^\circ C} Er_2O_2CN_2 + 4\ HCp \quad (4)$$

The overall yield of $Er_2O_2CN_2$ obtained in four reaction steps based on Cp_3Er as starting material [Eqs. (1)–(4)] is 25.6 mol%. In brief, we were able to synthesize pure lanthanide dioxo monocarbodiimides starting from ammonia and CO_2 by employing the well-known Cp_3Ln complexes as molecular precursors [Eq. (5)]. The oxophilic character of the lanthanides is the driving force for the reaction.

$$2\ Cp_3Er + 2\ NH_3 + CO_2 \longrightarrow Er_2O_2CN_2 + 6\ HCp \quad (5)$$

Synthesis and characterization of 3: For the synthesis of a crystalline carbamate complex, *tert*-butyl carbamate was considered as an appropriate ligand as it is easily available and has an unprotected amine moiety. Earlier pyrolysis reactions with *N*-alkylated lanthanide carbamato complexes such as $Eu_4(O_2CN\mathit{i}Pr_2)_{12}$ resulted in formation of spurious byproducts.[43] As illustrated in Scheme 1, Cp_3Ho reacts with one equivalent of *tert*-butyl carbamate in toluene to give

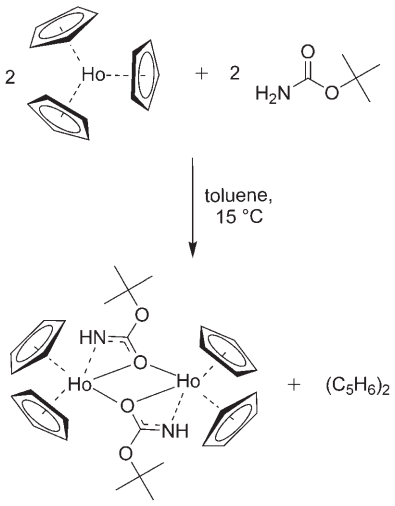

3

Scheme 1. Reaction of Cp_3Ho with *tert*-butyl carbamate to form **3**.

$[Ho_2\{\mu\text{-}\eta^1\text{:}\eta^2\text{-}OC(OtBu)NH\}_2Cp_4]$ (**3**), as determined by X-ray crystal structure analysis (Figure 5).

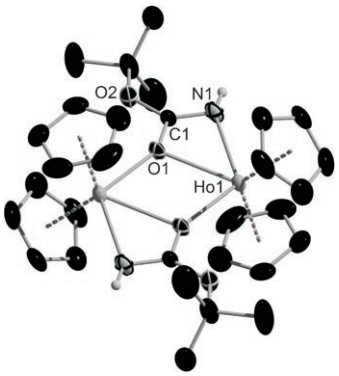

Figure 5. Molecular structure of **3** at 130 K (50% probability ellipsoids). Hydrogen atoms except NH are omitted for clarity.

Details of the structure refinement are summarized in Table 2. The atomic coordinates, anisotropic displacement parameters, and bond lengths and angles of **3** are given in the Supporting Information. The unit cell contains two crystallographically independent $[Ho_2\{\mu\text{-}\eta^1\text{:}\eta^2\text{-}OC(OtBu)NH\}_2Cp_4]$ moieties and two toluene molecules. Hydrogen atoms were calculated (CH) or unequivocally found in the difference Fourier map (NH) and refined with fixed isotropic thermal parameters.

The X-ray structure analysis reveals an unusual bonding mode of the carbamato ligand, which acts as both a bridging and side-on chelating group. Due to delocalization of the O-C-N fragment, the O1–C1 and C1–N1 distances of 1.297(5) and 1.285(6) Å, respectively, are between single- and double-bond lengths.[44] Each Ho atom is coordinated by two Cp groups, one chelating O-C-N fragment, and one bridging oxygen atom from another carbamato ligand. The Cp rings are perpendicular to the coplanar carbamato ligands. The distances between the Cp rings and the lanthanide atoms, as well as between the bridging oxygen and lanthanide atoms, correspond well with the expected ranges given in the literature for dimeric LnCp complexes.[45] The Ho1–N1 distance of 2.408(4) Å is slightly shorter than a Ho–N donor bond[10] and underlines the electronic delocalization of the O-C-N group. The IR spectrum of **3** is depicted in Figure 6.

Table 2. Crystallographic data for **3**.

formula	$C_{30}H_{40}HoN_2O_2{\cdot}C_7H_8$
M [g mol^{-1}]	914.65
crystal system	triclinic
space group	$P\bar{1}$
diffractometer	STOE IPDS Single Crystal
$\lambda(MoK_{\alpha1})$ [Å]	0.71073
T [K]	130
a [Å]	10.442(2)
b [Å]	13.085(3)
c [Å]	13.817(3)
α [°]	90.95(3)
β [°]	91.11(3)
γ [°]	110.26(3)
V [Å^3]	1770.3(6)
Z	2
ρ_{calcd} [g cm^{-3}]	1.716
$F(000)$	900
μ [mm^{-1}	4.477
crystal size [mm^3]	$0.33\times0.17\times0.1$
diffraction range	$2.95\le\theta\le30.44$
index range	$-14\le h=14$, $-18\le k\le18$, $-19\le l\le19$
total reflections	21017
independent reflections	9686 ($R_{int}=0.0345$)
observed reflections	6952
refined parameters	387
absorption correction	multiscan
min./max. transmission ratio	0.422/0.647
min./max. residual electron density [e Å^{-3}]	−1.184/1.654
GoF	0.922
final R indices [$I>2\sigma(I)$]	$R1=0.0302$, $wR2=0.671$
R indices (all data)	$R1=0.0515$, $wR2=0.0725$[a]

[a] $w=[\sigma^2(F_o^2)+(0.0411P)^2+0.00P]^{-1}$ where $P=(F_o^2+2F_c^2)/3$.

The characteristic absorption bands of the Cp ligand can be found at 3091, 1013, 790, and 770 cm^{-1}. The signals at 3519 and 3404 cm^{-1} can be identified as N–H stretching vi-

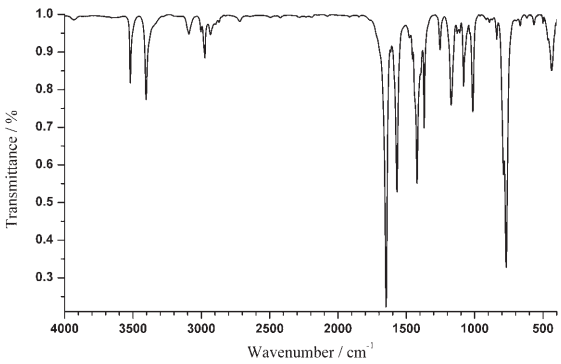

Figure 6. FTIR spectrum of **3** recorded as KBr pellet between 400 and 4000 cm^{-1}.

brations, and the bands at 2974 and 2933 cm^{-1} as C–H stretching frequencies of the *tert*-butyl group. The absorption at 1569 cm^{-1} can be assigned to the delocalized mode of the O-C-N fragment, according to literature data.[44,46] Considering the broader absorptions for amorphous compounds the signals in the region between 1650 and 1400 cm^{-1} correspond well with those of the CO_2 insertion products mentioned above (Figure 1). Therefore, the IR data of **3** add another piece of evidence for formation of carbamate compounds by insertion of CO_2 into lanthanide amido complexes.

Crystalline **3** was obtained by recrystallization from cold toluene, which decreased the yield to 50% based on Cp_3Ho. An amorphous precursor with identical composition and pyrolysis behavior can be obtained in nearly quantitative yield by stirring Cp_3Ho and *tert*-butyl carbamate in toluene and subsequently removing the solvent. Consequently, the following reactions were carried out using the amorphous derivative of **3** (**3a**).

Pyrolysis of 3a: Temperature-programmed XRPD patterns of **3** recorded under inert gas atmosphere indicated X-ray amorphous character of the intermediate product above 50 °C. This observation is supported by the TG/DTA measurements indicating the onset of the decomposition at 45 °C accompanied by an endothermic DTA signal. The TG/DTA measurements were performed analogously to those for **2** and afforded Ho_2O_3 under a nonreducing atmosphere. The ion flow has two maxima between 100 and 130 °C, which consisting mostly of fragments of the *tert*-butyl group (e.g., isobutene) and the Cp ligands. In the region between 150 and 200 °C CO_2 is the prevailing species. These events are also indicated by the DSC curve (Figure 7) as endothermic features at 114, 128, and 150 °C, respectively. Above 200 °C the TG/DTA measurements provide no significant information, which is also in accordance with the DSC curve.

Ammonolysis of **3a** in a manner analogous to **2** afforded phase-pure and crystalline $Ho_2O_2CN_2$, as proven by elemental analysis, FTIR spectroscopy, and Rietveld refinement.

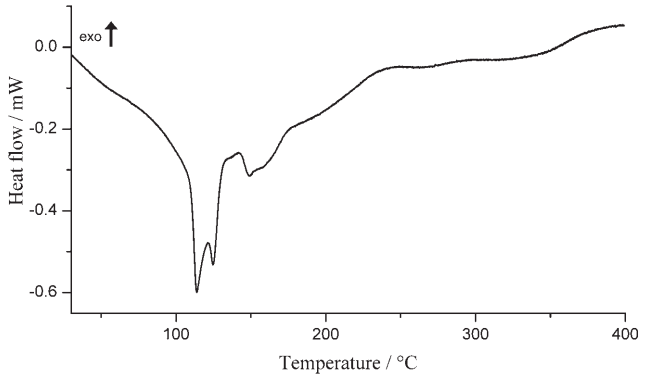

Figure 7. Differential scanning calorimetry of **3a** between room temperature and 400 °C. The significant thermal events at 114 and 128 °C can be attributed to loss of the cyclopentadienyl rings and the *tert*-butyl group. The signal at 150 °C results from released CO_2.

Details of the structure determination are summarized in Table 1. The Rietveld plot, atom positions, and isotropic displacement parameters of $Ho_2O_2CN_2$ can be found in the Supporting Information.

Starting from **3a** we were able to increase the yield to 66% with respect to Cp_3Ho. Based on the gaseous pyrolysis products detected during the TG/DTA measurements, the ammonolysis reaction yielding dioxo monocarbodiimides can be formulated as Equation (6).

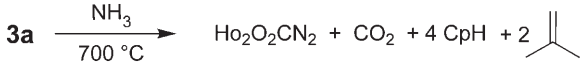

(6)

TG/DTA measurements carried out for $Ho_2O_2CN_2$ from room temperature to 1400 °C under He atmosphere indicate its decomposition around 1020 °C by an endothermic DTA signal. The final pyrolysis product was analyzed by XRPD and found to consist of Ho_2O_3 and HoN. Hence, $Ho_2O_2CN_2$ continues the trend of a remarkable increase in degradation temperature with decreasing ionic radius of the lanthanide, as reported for known dioxo monocarbodiimides.[16]

The same approach was also applied to the synthesis of $Er_2O_2CN_2$ and to $Y_2O_2CN_2$, which recently has been described in the literature,[26] and gave the desired products in good yields and phase-pure, as proven by XRPD. On extending the synthesis to $Yb_2O_2CN_2$, the resulting powder pattern showed another unidentified phase. Investigations are presently underway to characterize and understand the formation of the byproduct and thereafter clarify the structural parameters of $Yb_2O_2CN_2$. Until now, Er is the heaviest rare earth element to form phase pure dioxo monocarbodiimides $Ln_2O_2CN_2$.

Conclusion

We were able to utilize CO_2 as a preorganized C/O donor for the synthesis of novel O/C/N-containing lanthanide carbamate precursors. Insertion of CO_2 into lanthanide amido complex **1** forming a lanthanide carbamate "single-source" precursor with the formula $[Er_2(O_2CN_2H_4)Cp_4]$ has been investigated. Furthermore, the amount of CO_2 inserted can be controlled by the supercritical reaction conditions. Decomposition of **2** was investigated by TG/DTA, DSC, and mass spectrometry. Ammonolysis of **2** by employing a LiCl/KCl flux yielded highly crystalline and phase-pure dioxo monocarbodiimide $Er_2O_2CN_2$, whose crystal structure was refined based on XRPD data by the Rietveld method. Therefore, we were able to use the insertion of CO_2 into organic precursors to obtain new solid-state compounds. As demonstrated above, labile carbamate intermediates turned out to be excellent starting materials for the synthesis of hitherto-unavailable species in the system Ln/O/C/N. Additionally, we developed a straightforward pathway using a classical precursor route with preorganization at the metal center.

Thus, crystalline lanthanide *tert*-butyl carbamato complex **3** was synthesized and fully characterized. Ammonolysis of **3a** yielded phase-pure $Ho_2O_2CN_2$ with significantly improved yields. This pathway was successfully applied to $Y_2O_2CN_2$, $Er_2O_2CN_2$, and $Yb_2O_2CN_2$, whereas $Er_2O_2CN_2$ represents the present borderline for the phase-pure synthesis of lanthanide dioxo monocarbodiimides. The present study shows that the oxophilicity of the well known Cp_3Ln complexes can be utilized to bind gaseous reactants such as CO_2 or ammonia and thus use them for tailor-made precursor design in the synthesis of solid-state materials to form compounds which are inaccessible by standard routes. $Y_2O_2CN_2$ as host lattice in combination with $Er_2O_2CN_2$ as dopant has potential for the synthesis of new sorts of NIR phosphors.

Experimental Section

Unless otherwise stated, all manipulations were performed with rigorous exclusion of oxygen and moisture in flame-dried Schlenk-type glassware on a Schlenk line interfaced to a vacuum line (10^{-3} mbar) or in an argon-filled glovebox. Argon was purified by passage over columns of silica gel, molecular sieves, KOH, P_4O_{10}, and titanium sponge (700 °C). Ammonia was predried by passage over columns of KOH and Cr^{II} oxide catalyst,[47] and then condensed and stored over Na and K before use. Toluene was refluxed and distilled over $LiAlH_4$ under argon immediately prior to use. Cp_3Ln compounds (Ln = Y, La, Ho, Er, Yb) were prepared according to well-known procedures[48] and sublimed twice before use (10^{-3} mbar, 120–250 °C). Further treatment of Cp_3Er in liquid ammonia and subsequent pyrolysis afforded **1** according to recent investigations.[10] CO_2 was of 4.5 grade (Air Liquide). *tert*-Butyl carbamate was purchased from Alfa Aesar and used without purification.

General procedure for reactions in supercritical CO_2: The starting material was introduced into a Parr high-pressure vessel (Type 4740) with a Parr gage block (Type 4316) and connected to a gas vacuum line. Carbon dioxide was desublimed by cooling the vessel to −80 °C until sufficient solid CO_2 was present. The reaction vessel was closed and warmed slowly to the desired temperature. A pressure of 220–280 bar was observed during the reaction. After two days, the pressure was reduced carefully by opening the valve of the unit and the vessel was opened in an argon-filled glove box. An orange powder was isolated and analyzed by IR spectroscopy and elemental analysis.

$[Er_2(O_2CN_2H_4)Cp_4]$ (2): $[(Cp_2ErNH_2)_2]$ (300 mg, 0.48 mmol); reaction temperature 50 °C, 3 days, pressure 220 bar, orange powder. Yield: 257.6 mg (80 %). Elemental analysis calcd (%) for **2** (670.1): C 37.6, H 3.6, N 4.2, O 4.8, Er 49.9; found: C 37.4, H 3.77, N 4.2, O 4.5, Er 49.6. IR (KBr): $\tilde{\nu}$ = 3501 (m), 3479 (m), 3381 (m), 3300 (m), 3225 (m), 3088 (w), 3070 (sh), 1621 (s), 1554 (s), 1452 (s), 1357 (m), 1289 (m), 1122 (vw), 1084 (w), 1058 (m), 1010 (s), 890 (vw), 783 (s), 773 (sh), 715 (m), 683 (m), 451 cm^{-1} (m).

$[Er_2(O_2CNH_2)_2(CO_2)_3Cp_4]$: $[(Cp_2ErNH_2)_2]$ (300 mg, 0.48 mmol), reaction temperature 150 °C, 4 days, pressure 220 bar, orange powder. Elemental analysis calcd (%) for $[Er_2(O_2CNH_2)_2](CO_2)_3Cp_4]$ (847.0): C 35.5, H 2.9, N 3.3, O 18.9, Er 39.5; found: C 32.6, H 2.7, N 3.2, O 19.0, Er 40.0. IR (KBr): $\tilde{\nu}$ = 3501 (w), 3378 (w), 3060 (vw), 2965 (w), 2936 (w), 1628 (vs), 1532 (vs), 1429 (vs), 1290 (s), 1132 (w), 1058 (w), 1012 (w), 892 (vw), 782 (m), 737 (m), 715 (m), 468 (w), 430 cm^{-1} (w).

$[Ho_2\{\mu\text{-}\eta^1{:}\eta^2\text{-}OC(OtBu)NH\}Cp_4]$ (3): A solution of *tert*-butyl carbamate (87.8 mg, 0.75 mmol) in toluene (3 mL) was added to a suspension of Cp_3Ho (270 mg, 0.75 mmol) in toluene (15 mL) at 15 °C. After stirring for 1 h, the mixture was cooled to 6 °C for 16 h to give **3** as orange crystals. Yield: 165 mg (54 %). IR (KBr): $\tilde{\nu}$ = 3519 (w), 3404 (w), 3091 (vw), 2973 (w), 2933 (vw), 1648 (vs), 1569 (m), 1422 (m), 1370 (w), 1254 (w), 1172 (w), 1081 (w) 1013 (w), 790 (m), 770 (s), 435 cm^{-1} (w).

General procedure for the pyrolysis reaction leading to $Ln_2O_2CN_2$: The precursor was ground in a mortar, placed in a dry alumina boat and transferred to a silica tube which was connected to a Schlenk line. The silica tube was heated in a Reetz collapsible tube furnace (LK-1100-45-250) controlled by an Omron (RE.LB.1.P16) temperature controller. The solid was heated under vacuum to 120 °C to remove residual solvent. A flowing stream of dry ammonia gas was adjusted and the solid was heated (5 °C min^{-1}) to 250 °C. The temperature was maintained for 2 h. A change in color and a weight loss of approximately 50 % were observed. Afterwards the alumina boat was cooled to room temperature and transferred to a glove box. The solid was ground together with the same amount of an eutectic mixture of dry LiCl and KCl. Subsequently, the reaction mixture was again transferred to the silica tube and heated (5 °C min^{-1}) under a stream of ammonia gas to 700 °C. After 2 h the ammonia stream was shut off and the temperature was maintained for 18 h. The product was washed twice with water to remove the flux.

$Er_2O_2CN_2$: Yield (54 %). Elemental analysis calcd (%) for $Er_2O_2CN_2$ (406.5): C 3.0, H 0.0, N 6.9, O 7.9, Er 82.3; found: C 3.0, H < 0.1, N 6.4, O 8.4, Er 81.4. IR (KBr): $\tilde{\nu}$ = 2157 (s), 652 (m), 447 cm^{-1} (s).

$Ho_2O_2CN_2$: Yield (66 %). Elemental analysis calcd (%) for $Ho_2O_2CN_2$ (401.9): C 3.0, H 0.0, N 7.0, O 8.0, Ho 82.0; found: C 3.0, H < 0.1, N 6.6, O 8.4, Ho 81.3. IR (KBr): $\tilde{\nu}$ = 2156 (s), 652 (m), 442 cm^{-1} (s).

Vibrational spectroscopy: FTIR measurements were carried out on a Bruker IFS 66v/S spectrometer. The preparation procedures were performed in a glove box under dried argon atmosphere. Spectra were recorded at ambient conditions in the range between 400 and 4000 cm^{-1} by dispersing the samples in anhydrous KBr pellets.

Elemental analysis: Elemental analysis was performed by Mikroanalytisches Labor Pascher, Remagen, Germany. Each element of the sample was analyzed twice.

Thermal analysis: TG/DTA measurements were performed on a simultaneous thermogravimetry/differential thermal analyzer (Netzsch STA 409 CD) coupled with a quadrupole mass spectrometer (Pfeiffer Vacuum OMG 422). The sample was heated from RT to 1400 °C at a heating rate of 1 °C min^{-1} in an alumina crucible (gas flow 100 mL min^{-1} helium 5.0). The DSC measurements were carried out in an aluminum crucible on a Setaram DSC 141 for **2** and a Netzsch DSC 204 Phoenix for **3a**.

X-ray diffraction: Single-crystal X-ray data were collected on a STOE IPDS diffractometer ($Mo_{K\alpha}$ radiation). The program package SHELX97 was used for structure solution and refinement.[49] CCDC 658159 contains the supplementary crystallographic data for this paper. These data can be obtained free of charge from The Cambridge Crystallographic Data Centre via www.ccdc.cam.ac.uk/data_request/cif.

Powder diffraction data were collected in Debye–Scherrer geometry on a STOE Stadi P powder diffractometer with Ge(111)-monochromatized $Cu_{K\alpha1}$ radiation (λ = 1.5406 Å) for $Er_2O_2CN_2$ and on a Huber Imaging Plate Guinier diffractometer G670 for $Ho_2O_2CN_2$. For pattern fitting (Le Bail algorithm) and Rietveld refinements the GSAS[41] program package and EXPGUI[50] were used. Further details of the crystal structure investigations can be obtained from the Fachinformationszentrum Karlsruhe, 76344 Eggenstein-Leopoldshafen, Germany (fax: (+49)7247-808-666; e-mail: crysdata@fiz-karlsruhe.de) on quoting the depository numbers CSD-418478 ($Er_2O_2CN_2$) and CSD-418477 ($Ho_2O_2CN_2$).

High-temperature in situ X-ray diffractometry was performed on a STOE Stadi P powder diffractometer (Ge(111)-monochromated $Mo_{K\alpha1}$ radiation, λ = 71.037 pm) in an integrated furnace with sealed silica capillaries ($\varnothing$ 0.3 mm) as sample containers. Data collection was restricted to a 2θ range of 5–22° and a single scan collection time of 20 min. The samples were heated from 20 to 800 °C in steps of 50 °C at a heating rate of 1.3 °C min^{-1}.

Acknowledgements

The authors are indebted to the following people for conducting the physical measurements: Christoph Schneck (simultaneous thermal analy-

sis and DSC measurements, group of Prof. Schleid, Institute of Inorganic Chemistry, University Stuttgart), Wolfgang Wünschheim (DSC measurements), Dr. Oliver Oeckler, Thomas Miller (single-crystal X-ray diffractometry) (all Department of Chemistry and Biochemistry, LMU Munich); and Dr. Bettina V. Lotsch (Prof. Dr. G. Ozin Group, Department of Chemistry, University Toronto) and Dr. Ulrich Baisch (Group of Prof. Dr. D. Braga, Università di Bologna) are thanked for lively discussions. Financial support from the Deutsche Forschungsgemeinschaft (DFG) (Schwerpunktprogramm SPP 1166, Lanthanoidspezifische Funktionalitäten in Molekül und Material, project SCHN377/10) and the Fonds der Chemischen Industrie is also gratefully acknowledged.

[1] J. W. Stouwdam, F. C. J. M. van Veggel, *ChemPhysChem* **2004**, *5*, 743.
[2] T. C. Kirk, E. G. Lundquist, T. R. Lynn (Rohm & Haas, USA), EP 1367070, **2003**; [*Chem. Abstr.* **2003**, *139*, 396303].
[3] G. A. Molander, J. A. C. Romero, *Chem. Rev.* **2002**, *102*, 2161.
[4] R. E. Murray (Union Carbide Chem. Plastic, USA), WO 9901460, **1999**; [*Chem. Abstr.* **1999**, *130*, 125530].
[5] D. Hanaoka, S. Ito (Sharp Corp., Japan), JP 2001148540, **2001**; [*Chem. Abstr.* **2001**, *134*, 373859].
[6] M. Martens, *Ingenieursblad* **1971**, *40*, 287.
[7] H. Tanaka, M. Hashimoto, S. Emura, A. Yanase, R. Asano, Y. K. Zhou, H. Bang, K. Akimoto, T. Honma, N. Umesaki, H. Asahi, *Phys. Status Solidi C* **2003**, 2864.
[8] R. Mueller-Mach, G. Mueller, M. R. Krames, H. A. Höppe, F. Stadler, W. Schnick, T. Juestel, P. Schmidt, *Phys. Status Solidi A* **2005**, *202*, 1727.
[9] T. Juestel, P. Schmidt, H. Höppe, W. Schnick, W. Mayr (Philips Intellectual Property & Standards GmbH, Germany; Koninklijke Philips Electronics N.V.; Lumileds Lighting U.S. Llc), WO 2004055910, **2004**; [*Chem. Abstr.* **2004**, *141*, 96377].
[10] U. Baisch, S. Pagano, M. Zeuner, N. Barros, L. Maron, W. Schnick, *Chem. Eur. J.* **2006**, *12*, 4785.
[11] U. Baisch, S. Pagano, M. Zeuner, J. Schmedt auf der Günne, O. Oeckler, W. Schnick, *Organometallics* **2006**, *25*, 3027.
[12] H. A. Höppe, F. Stadler, O. Oeckler, W. Schnick, *Angew. Chem.* **2004**, *116*, 5656; *Angew. Chem. Int. Ed.* **2004**, *43*, 5540.
[13] W. Schnick, R. Bettenhausen, B. Götze, H. A. Höppe, H. Huppertz, E. Irran, K. Köllisch, R. Lauterbach, M. Orth, S. Rannabauer, T. Schlieper, B. Schwarze, F. Wester, *Z. Anorg. Allg. Chem.* **2003**, *629*, 902.
[14] F. Stadler, W. Schnick, *Z. Anorg. Allg. Chem.* **2006**, *632*, 949.
[15] U. Baisch, S. Pagano, M. Zeuner, W. Schnick, *Eur. J. Inorg. Chem.* **2006**, 3517.
[16] Y. Hashimoto, M. Takahashi, S. Kikkawa, F. Kanamaru, *J. Solid State Chem.* **1996**, *125*, 37.
[17] Y. Hashimoto, M. Takahashi, S. Kikkawa, F. Kanamaru, *J. Solid State Chem.* **1995**, *114*, 592.
[18] G. W. Ludwig, J. S. Prener, *IEEE Trans. Nucl. Sci.* **1972**, *19*, 415.
[19] W. H. Fronger, C. W. Struck, *J. Electrochem. Soc.* **1971**, *118*, 273.
[20] M. Takahashi, Y. Hashimoto, S. Kikkawa, H. Kobayashi, *Zairyo* **2000**, *49*, 1230.
[21] J. Holsa, R.-J. Lamminmaki, M. Lastusaari, P. Porcher, E. Sailynoja, *J. Alloys Compd.* **1998**, *275–277*, 402.
[22] J. Holsa, R. J. Lamminmaki, M. Lastusaari, E. Sailynoja, P. Porcher, P. Deren, W. Strek, *Spectrochim. Acta Part A:* **1998**, *54*, 2065.
[23] E. Saeilynoja, M. Lastusaari, J. Hoelsaea, P. Porcher, *J. Lumin.* **1997**, *72*, 201.
[24] P. Caro, *J. Less-Common Met.* **1968**, *16*, 367.
[25] T. Takeda, N. Hatta, S. Kikkawa, *Chem. Lett.* **2006**, *35*, 988.
[26] J. Sindlinger, J. Glaser, H. Bettentrup, T. Jüstel, H.-J. Meyer, *Z. Anorg. Allg. Chem.* **2007**, *633*, 1686.
[27] R. Srinivasan, S. Tragl, H.-J. Meyer, *Z. Anorg. Allg. Chem.* **2005**, *631*, 719.
[28] O. Reckeweg, F. J. DiSalvo, *Angew. Chem.* **2000**, *112*, 397; *Angew. Chem. Int. Ed.* **2000**, *39*, 412.
[29] U. Berger, W. Schnick, *J. Alloys Compd.* **1994**, *206*, 179.
[30] B. Jürgens, W. Milius, P. Morys, W. Schnick, *Z. Anorg. Allg. Chem.* **1998**, *624*, 91.
[31] M. Krott, X. Liu, B. P. T. Fokwa, M. Speldrich, H. Lueken, R. Dronskowski, *Inorg. Chem.* **2007**, *46*, 2204.
[32] X. Liu, M. Krott, P. Mueller, C. Hu, H. Lueken, R. Dronskowski, *Inorg. Chem.* **2005**, *44*, 3001.
[33] H. Fischer, Dissertation, TU München **1965**.
[34] H. P. Fritz, *Adv. Organomet. Chem.* **1964**, *1*, 239.
[35] W. J. Evans, J. M. Perotti, S. A. Kozimor, T. M. Champagne, B. L. Davis, G. W. Nyce, C. H. Fujimoto, R. D. Clark, M. A. Johnston, J. W. Ziller, *Organometallics* **2005**, *24*, 3916.
[36] F. A. Cotton, T. J. Marks, *J. Am. Chem. Soc.* **1969**, *91*, 7281.
[37] T. Okamura, K. Sakauye, N. Ueyama, A. Nakamura, *Inorg. Chem.* **1998**, *37*, 6731.
[38] U. Baisch, D. Belli Dell′Amico, F. Calderazzo, L. Labella, F. Marchetti, A. Merigo, *Eur. J. Inorg. Chem.* **2004**, 1219.
[39] M. Neukirch, S. Tragl, H.-J. Meyer, *Inorg. Chem.* **2006**, *45*, 8188.
[40] R. Srinivasan, J. Glaser, S. Tragl, H.-J. Meyer, *Z. Anorg. Allg. Chem.* **2005**, *631*, 479.
[41] A. C. Larson, R. B. Von Dreele, General Structure Analysis System (GSAS), 86-748, Los Alamos National Laboratory Report LAUR: 2000.
[42] U. Berger, W. Schnick, *Z. Anorg. Allg. Chem.* **1995**, *621*, 2075.
[43] U. Baisch, Dissertation, LMU München **2006**.
[44] X. Zhou, L. Zhang, M. Zhu, R. Cai, L. Weng, *Organometallics* **2001**, *20*, 5700.
[45] H. Schumann, J. A. Meese-Marktscheffel, L. Esser, *Chem. Rev.* **1995**, *95*, 865.
[46] J. D. Wilkins, *J. Organomet. Chem.* **1974**, *67*, 269.
[47] H. L. Krauss, H. Stach, *Z. Anorg. Allg. Chem.* **1969**, *366*, 34.
[48] W. A. Herrmann, *Synthetic Methods of Organometallic and Inorganic Chemistry, Vol. 6*, 1st ed., Thieme, Stuttgart, New York, **1996**.
[49] G. M. Sheldrick, SHELX97, Program package for the solution and refinement of crystal structures, Release 97-2, University of Göttingen, Germany, **1997**.
[50] EXPGUI, a graphical user interface for GSAS: B. H. Toby, *J. Appl. Crystallogr.* **2001**, *34*, 210–213.

Received: August 23, 2007
Revised: October 17, 2007
Published online: December 3, 2007

